[American Journal of Science, Vol. 305, February, 2005, P. 101–118]

American Journal of Science

FEBRUARY 2005

STABLE ISOTOPE RECORDS OF CENOZOIC CLIMATE AND TOPOGRAPHY, TIBETAN PLATEAU AND TARIM BASIN

STEPHAN A. GRAHAM*†, C. PAGE CHAMBERLAIN*, YONGJUN YUE*, BRADLEY D. RITTS**, ANDREW D. HANSON***, TRAVIS W. HORTON*, JACOB R. WALDBAUER*, MICHAEL A. POAGE****, and X. FENG****

ABSTRACT. We seek to better understand growth of the Tibetan plateau and associated climate change by presenting the first regionally extensive set of oxygen isotope data obtained from ca. 40 m.y. of Cenozoic strata from a 700,000 km^2 area ranging from the northern edge of the Tibetan plateau northward across the entire Tarim basin. Our results reveal a previously unrecognized large positive isotope shift from Eocene to Oligocene which we suggest results from initial topographic growth of the Himalayan-Tibetan system and attendant reorganization of climate by this growing mountain belt. A negative isotopic shift recorded in Miocene strata may reflect retreat of the Neotethyan Sea from the Tarim basin, as well as enhanced elevation of the Himalaya/Tibetan plateau region and the rise of the Tian Shan, which diverted moisture-bearing Westerlies and deepened aridity in the Tarim basin and the northern Tibetan plateau.

INTRODUCTION

The relationship between mountain building, plateau growth and climate change has been a dynamic and controversial topic over the past 15 years (Quade and others, 1989; Ruddiman and Kutzbach, 1990; Molnar and others, 1993; Stern and others, 1997; Chamberlain and Poage, 2000; Garizone and others, 2000; Rowley and others, 2001; Dettman and others, 2001, 2003). Especially important insights have been gleaned from the Himalaya/Tibet system, where oxygen isotopic shifts recorded in fossils, paleosol carbonate and smectite of the Indo-Gangaetic foreland basin south of the mountains were initially interpreted to reflect uplift of the Himalaya and initiation of monsoonal climate 8.5 to 6.5 Ma (Quade and others, 1989) and later reinterpreted to indicate that the monsoonal system was active by at least 10.7 Ma (Dettman and others, 2001). However, the current extreme contrast between the monsoon-dominated climate south of the Himalaya/Tibetan plateau (ca. 6 km elevation) (Molnar and others, 1993) and the extremely arid climate (<100 mm/yr precipitation) (Domros and Peng, 1984) of the vast, relatively low standing (ca. 1 – 1.5 km) Tarim basin north of the plateau (fig. 1) suggest that Cenozoic strata of the Tarim basin might contain an important record of uplift of the Tibetan plateau and attendant long-term climate change (aridification). Such a record, if it exists, might provide important constraints on controversial models of growth of the Tibetan plateau (Molnar and others, 1993; Tapponnier and others, 2001), which in turn more

* Department of Geological and Environmental Sciences, Stanford University, California 94305-2115, USA
** Department of Geological Sciences, Indiana University, Bloomington, Indiana 47405, USA
*** Department of Geological Sciences, University of Nevada, Las Vegas, Nevada 89154-4010, USA
**** Department of Earth Sciences, Dartmouth College, Hanover, New Hampshire 03755, USA
† Corresponding author: email: graham@pangea.stanford.edu; phone: (650) 723-0507; fax: (650) 725-0979

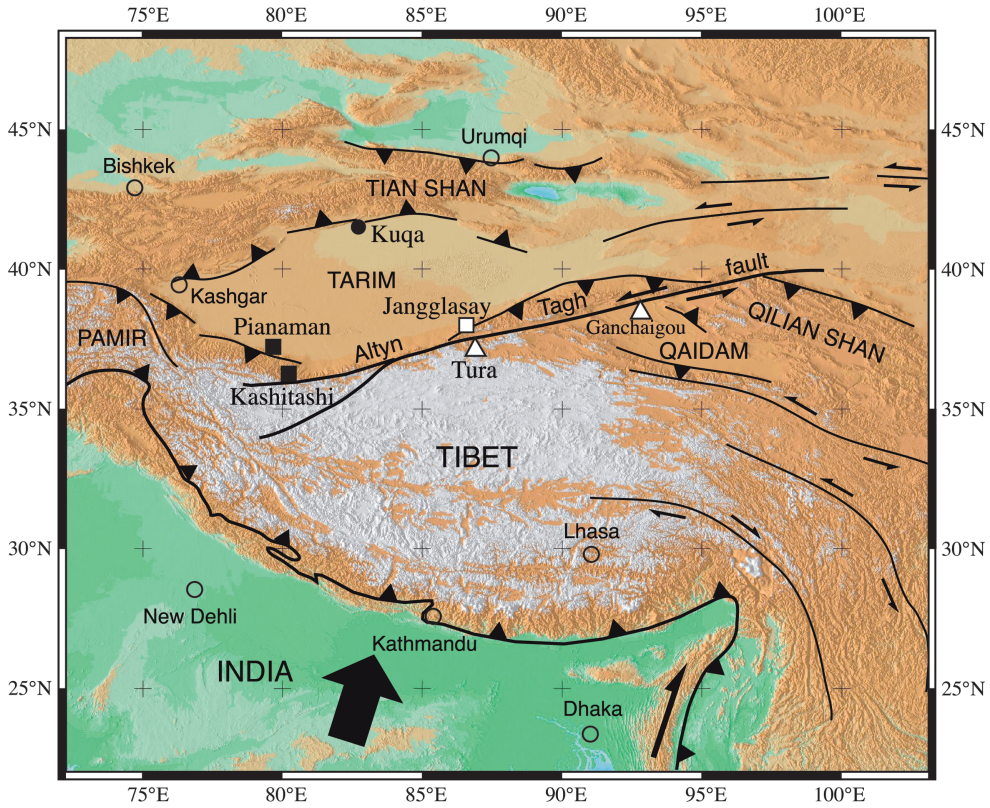

Fig. 1. Topography and principal active faults of Tibet and adjacent regions. Barbed lines are thrust faults. Bold lines with opposite arrows are strike-slip faults. The large filled arrow in India indicates motion of the sub-continent. Open circles are selected cities. Oxygen isotope sampling localities: Northern Tarim basin = solid circle; southern Tarim basin = solid squares; southeastern Tarim basin = open square; northern Tibet plateau = open triangles.

generally bears on considerations of how and at what rate deformation associated with collisional orogenesis propagates into continental interiors.

Surprisingly, few oxygen isotopic data have been published for Cenozoic strata from the Tibetan plateau. The extant pioneering Tibet studies are extremely important, but they derive from limited local areas of Nepal (Garizone and others, 2000; data reported in Rowley and others, 2001), the Linxia basin of eastern Tibetan plateau (Dettman and others, 2003), an unspecified locality in Qaidam basin (Rieser and others, 2003), and the Janggalsay area of southeastern Tarim basin (Chen and others, 2002), so cannot in of themselves provide a regional perspective on plateau uplift and climate change.

In this paper, we present a regionally extensive set of oxygen isotope data obtained from ca. 40 m.y. of Cenozoic strata from a 700,000 km^2 area ranging from the northern edge of the Tibetan plateau northward across the entire Tarim basin. The results reveal a previously unrecognized large positive isotope shift from Eocene to Oligocene, which we suggest results from initial topographic growth of the Himalayan-Tibetan system and attendant reorganization of climate by this growing mountain belt. A negative isotopic shift recorded in Miocene strata may reflect retreat of the Neotethyan Sea from the Tarim basin, as well as enhanced elevation of the Himalaya/Tibetan plateau

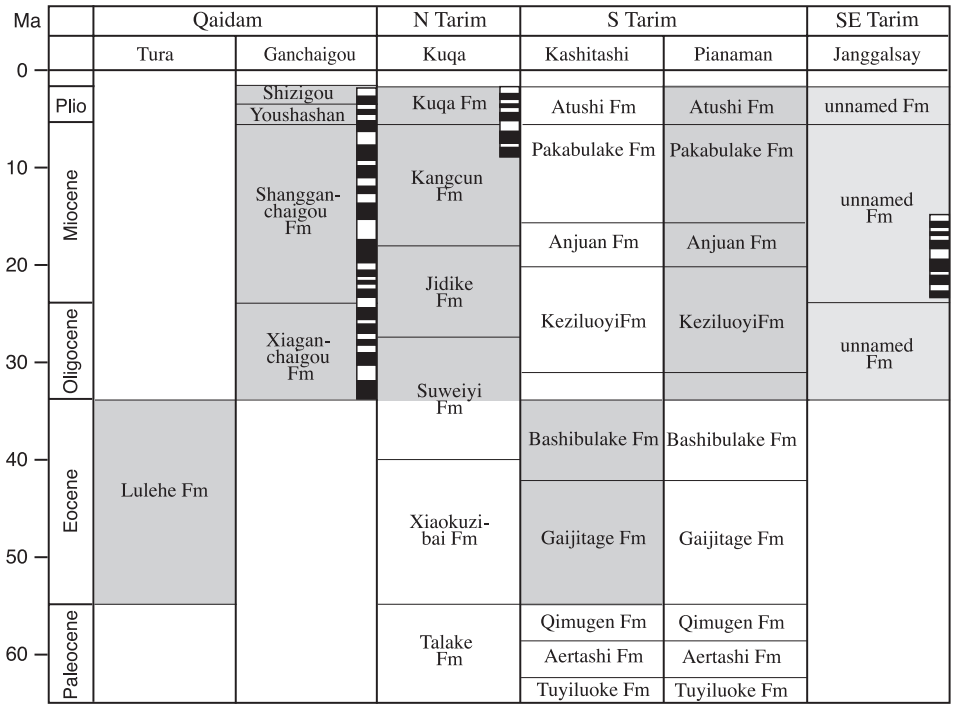

Fig. 2. Stratigraphy of Qaidam and Tarim basins. Gray areas indicate sections sampled in this study; black and white stripes indicate paleomagnetic polarity coverage. Sources of information: Sun and others (2004), XBGMR (1993), Yang and others (1994), Gilder and others (2001), Yin and others (2002), Zheng and others (2000), Zhou and Chen (1990), Wang and others (2003), Yue and others (2004a, 2004b).

region and the rise of the Tian Shan, which diverted moisture-bearing Westerlies and deepened aridity in the Tarim basin and the northern Tibetan plateau.

GEOLOGIC SETTING

The modern Qaidam and Tarim basins are internally drained, intermontane basins in western China (fig. 1). These basins evolved as collisional successor basins during the Mesozoic-Cenozoic history of tectonic amalgamation of southern Asia (Graham and others, 1993). Both were at or near sea level in the Mesozoic and likely were contiguous (Ritts, ms, 1998; Ritts and Biffi, 2000), but at some still undetermined time in the Cenozoic, the two basins became topographically distinct (Hanson, ms, 1999). The two basins currently are surrounded by high mountain belts, are separated from one another by the Altyn Tagh strike-slip fault, and on average differ in elevation by 2000 m. With the exception of the easternmost arm of the Neotethyan ocean that intruded episodically into the western half of Tarim basin during the Paleogene, both basins have been characterized by nonmarine alluvial, fluvial and lacustrine environments during the Cenozoic (Wang, 1985; Sobel, ms, 1995; Hanson, ms, 1999).

The chronostratigraphy of Cenozoic basin fill in the region is variably determined, but in general is much less well known than desirable due to lack of radiometrically datable stratigraphic units. This is an important issue for a chemostratigraphic study such we describe in this paper. Magnetostratigraphic records have been recovered from many Cenozoic basins of western China (fig. 2), but these in general suffer from uncertain correlations to the geologic time scale, giving rise to debate about their general utility in correlation and event timing.

Relatively arid environments characterized the Tarim-Qaidam region for much of the Cenozoic, so fossil biota are limited in some areas and for some time slices. For areas included in this study, age resolution of stratigraphic units and samples is at the epoch level.

Qaidam Basin

The Qaidam basin lies on the northern Tibet plateau at an average elevation of ~3000 m. It is bounded by the Altyn Tagh fault to the northwest and by thrust faults to the northeast and south (fig. 1). Mountainous topography surrounds the basin. Cenozoic sedimentation in the basin began in the Eocene, with deposition of a fluvial sequence composed of conglomerate, sandstone and lesser mudstone (Qinghai Bureau of Geology and Mineral Resources, 1991). Oligocene-Pliocene sedimentation occurred in fluvial and lacustrine environments, resulting in the deposition of a >5000 m thick assemblage of conglomerate, sandstone, paleosol carbonate, limestone and mudstone (Hanson, ms, 1999).

In this study, we sampled Eocene and Oligocene-Pliocene sections at Tura (86.9°E, 37.7°N) and Ganchaigou (92.8°E, 38.7°N), respectively (figs. 1, 2). The Eocene strata at Tura contain small, tridactyl vertebrate tracks; such mammal trackways occur in lower Tertiary rocks in Colorado, Utah and Peru (Ritts, ms, 1998; Lockley and others, 1999). The Oligocene to Pliocene strata at Ganchaigou contain abundant ostracods, pollen and algae and comprise the type section of the Qaidam basin (Gu and others, 1990; Qinghai Bureau of Geology and Mineral Resources, 1991; Yang and others, 1994; Hanson, ms, 1999).

Tarim Basin

The Tarim basin, bounded by the Altyn Tagh fault to the southeast and by thrust fault systems to the north and south, lies immediately north of the Tibet plateau and is the largest Cenozoic sedimentary basin in China (fig. 1). Tertiary strata at our Kuqa sampling locality (83°E, 42°N) in northern Tarim have a maximum thickness of 7000 meters (Yang and others, 1994). Paleocene-Eocene strata are redbeds deposited in fluvial-lacustrine environments with intercalated limestone, shale and gypsum beds deposited in shallow marine and lagoon environments, suggesting that the region was at sea level during that period of time (Sobel, ms, 1995). Oligocene to Pliocene strata consist of redbeds deposited in alluvial-fluvial-lacustrine environments (Zhou and Chen, 1990; Xinjiang Bureau of Geology and Mineral Resources, 1993; Yang and others, 1994).

Tertiary strata in southern Tarim are ~4000 meters thick. Paleogene and Miocene strata include nonmarine sandstone and mudstone, with lesser intercalated marine to lagoonal limestone and gypsum-bearing mudstone (Sobel, ms, 1995). However, at our sampling localities, Eocene strata at Kashitashi (80°E, 36.4°N) and Oligocene-Miocene strata at Pianaman (79.2°E, 37.1°N) consist of reddish to brownish mudstone with sandstone interbeds deposited in fluvial environments (Xinjiang Bureau of Geology and Mineral Resources, 1993; Hanson, ms, 1999). Pliocene strata are mainly conglomeratic rocks deposited in fluvial-alluvial environments. Tertiary strata in southeastern Tarim are 3000 to 4000 meters thick at Janggalsay (86.5°E, 38.1°N) (Hanson, ms, 1999; Yue and others, 2004a). Oligocene strata consist of interbedded mudstone, sandstone and conglomerate deposited in fluvial environments. The mudstone is highly calcareous and contains many horizons of nodular carbonate that we interpret as calcisols (compare Retallack, 1990; Mack and James, 1992). Miocene and Pliocene strata, also deposited in fluvial depositional environments, are conglomerate rich with a number of mudstone and fine-grained sandstone interbeds (Zhou and Chen, 1990; Hanson, ms, 1999; Yin and others, 2002; Yue and others, 2004a).

In this study, we sampled Oligocene-Pliocene sections from northern and southeastern Tarim, and an Eocene-Pliocene section in southern Tarim (fig. 1). The age assignment for the Oligocene-Pliocene strata in northern Tarim is mainly based on the ubiquitous occurrence of ostracods and algae throughout the section, and paleomagnetic polarity studies of the upper part of the section (fig. 2; Sun and others, 2004).

Tertiary strata in southern Tarim are relatively well dated because Paleocene to Miocene strata at most localities contain interbedded fossiliferous marine strata and because several paleomagnetic polarity studies have been conducted (Zheng and others, 2000; Yin and others, 2002). The Eocene age assignment of the strata at Kashitashi is mainly based on correlation with fossiliferous strata in the adjacent area (for example, Pianaman). The subdivision of Oligocene-Pliocene strata that overlie fossiliferous Eocene beds in Pianaman (Hanson, ms, 1999) is based on correlation with Oligocene-Pliocene strata to the west.

The age assignment for the Oligocene-Pliocene strata in southeastern Tarim is traditionally based on regional stratigraphic correlation. However, a recent paleomagnetic polarity study indicates that the lower part of the designated Miocene strata was either deposited near the Oligocene/Miocene boundary or the earliest Miocene (Yin and others, 2002). In addition, apatite fission-track analyses of sandstone samples collected from the designated Pliocene strata confirm that they were deposited after 10 Ma (Hanson, ms, 1999; Yue and others, 2004a). Both lines of new evidence support the previous age assignment based on a regional correlation.

METHODS

Stable Isotope Analyses

The analyses (tables 1, 2) were conducted in the Stable Isotope Biogeochemistry Laboratory at Stanford University. In this study we examined the oxygen and carbon isotopic composition of calcite from paleosol carbonate, lacustrine limestone and mudstone, and carbonate cement from fluvial sandstones. Although the interpretation of the isotopic values from these different rock types can be complicated by such factors as soil water evaporation (paleosols), and evaporation in lakes and streams (lacustrine limestones and cements) each of these systems has been shown to preserve long-term climate information (Cerling, 1984; Smith and Dorobeck, 1993; McKenzie and Hollander, 1993). Moreover, when these different climate proxies are used in concert in the same stratigraphic section they provide a redundancy that enhances the ability to extract long-term climate records (Horton and others, 2004).

A few milligrams of rock powder were obtained from samples using a dentist's drill. The powder was put into a sealed reaction vessel, which was later flushed with helium gas before adding pure phosphoric acid. Reaction between the acid and the rock powder at 70°C released carbon dioxide, whose isotopic ratios were measured using an automated gas bench coupled to a gas-ratio mass spectrometer (Finnigan MAT Delta Plus). The precision of these isotope measurements is ± 0.2 permil. Our data are reported relative to SMOW.

Petrographic Analyses

Petrographic analyses were performed on sandstone samples to calculate their intergranular volumes and the abundance of extrabasinal carbonate grains. All calculations are based on about 500 total points counted for each thin section (table 3). These points were classified as framework grains and interstitial material, the latter including cement, pore space and matrix. The intergranular volume of a sandstone sample is defined as the interstitial material volume divided by the total rock volume (Houseknecht, 1987; Paxton and others, 2002). The extrabasinal framework grain content of a sample is expressed in two ways: (1) the ratio of extrabasinal carbonate grains to the

TABLE 1

Oxygen Isotope Results

Region	Age	Sample	Lithology	δO^{18} *
Qaidam	Eocene	95TR327†	sandstone	21.3
		95TR329	sandstone	19.3
		95TR331	sandstone	18.4
		95TR333	sandstone	20.0
	Oligocene	95GC105	sandstone	22.8
		95GC106	sandstone	23.1
		95GC109	mudstone	25.0
		95GC110	calcrete	26.1
		95GC113	calcrete	25.3
		95GC114	sandstone	24.9
		95GC115	calcrete	26.8
		95GC116	calcrete	25.1
		95GC117	calcrete	24.8
		95GC119	mudstone	24.6
	Miocene	95GC122	sandstone	23.6
		95GC123	calcrete	26.6
		95GC124	mudstone	24.5
		95GC125	mudstone	28.2
	Pliocene	95GC127	mudstone	23.1
		95GC128	mudstone	22.9
		95GC129	sandstone	23.1
		95GC130	limestone	23.4
		95GC131	limestone	22.8
		95GC133	mudstone	23.1
		95GC134	mudstone	22.4
		95GC135	sandstone	23.2
		95GC136	sandstone	21.3
		95GC137	sandstone	23.1
		95GC138	sandstone	24.0
		95GC139	sandstone	22.3
Southern Tarim	Eocene	96RE100	sandstone	16.9
		96RE102	sandstone	15.4
		96RE103	sandstone	16.4
		96RE104	sandstone	17.7
		96RE105	sandstone	16.4
		96RE106	sandstone	15.4
		96RE107	sandstone	16.7
		96RE108	sandstone	16.0
		96RE109	sandstone	14.0
	Oligocene	96SH113	sandstone	18.2
		96SH114	sandstone	19.3
		96SH115	sandstone	20.0
	Miocene	96SH116	sandstone	19.7
		96SH117	sandstone	18.7
		96SH118	sandstone	18.9
		96SH119	sandstone	19.7
		96SH120	mudstone	19.8
	Pliocene	96SH121	sandstone	19.3
South-eastern Tarim	Oligocene	JA1	sandstone	19.3
		JA2	sandstone	20.5
	M.* and U. Miocene	JA3	sandstone	18.4
		JA4	sandstone	18.8
		JA5	sandstone	19.2
		JA6	sandstone	19.2
	Lower Pliocene	JA7	sandstone	15
		JA8	sandstone	15.8
		JA9	sandstone	16.4
		JA10	sandstone	16.7
		JA11	sandstone	17.0
	Upper Pliocene	JA12	sandstone	17.0
		JA13	sandstone	17.2
		JA14	sandstone	17.4
		JA15	sandstone	17.8
		JA16	sandstone	17.7
		JA17	sandstone	18.6
		JA18	sandstone	20.0
Northern Tarim	Oligocene	KQ1	sandstone	21.4
		KQ2	sandstone	21.5
		KQ3	sandstone	21.8
		KQ4	sandstone	22.2
	L. and M. Miocene	KQ5	sandstone	20.6
		KQ6	sandstone	20.6
		KQ7	sandstone	21.2
		KQ8	sandstone	21.8
		KQ9	sandstone	21.9
		KQ10	sandstone	22.0
		KQ11	sandstone	22.7
		KQ12	sandstone	22.8
		KQ13	sandstone	23.5
	Upper Miocene-Pliocene	KQ14	sandstone	19.5
		KQ15	sandstone	19.6
		KQ16	sandstone	19.8
		KQ17	sandstone	20.2
		KQ18	sandstone	20.8
		KQ19	sandstone	21.5
		KQ20	sandstone	21.7

* Relative to SMOW

† Abbreviations: TR: Tura, GC: Ganchaigou, SH: Pianaman, RE: Kashitashi, JA: Jangglasay, and KQ: Kuqa.

cement count, (2) ratio of extrabasinal carbonate grains to total framework grains (table 3).

Ion Microprobe Analyses

The Sr/Ca and Mg/Ca ratios of carbonate samples (table 4) were measured using the SHRIMP-RG at the Stanford-U.S. Geological Survey Microisotope Analytical Cen-

TABLE 2

T-Test Results for the Oxygen Isotope Data from Northern Tibet

Location	Age groups	μ_1	μ_2	n_1	n_2	ν_1	ν_2	t_c	t_t	t_c-t_t
Southern Tarim	Eocene/Oligocene	16.1	19.1	9	3	1.11	0.79	4.4	2.78	1.62
	Oligocene/Miocene	19.1	19.3	10	5	0.79	0.26	0.46	2.18	-1.72
Qaidam (Northern Tibet)	Eocene/Oligocene	19.7	24.8	4	10	1.54	1.44	7.12	2.57	4.55
	Oligocene/Miocene	24.8	25.7	10	4	1.44	4.22	1.04	3.18	-2.14
	Miocene/Pliocene	25.7	22.9	4	12	4.22	0.46	4.31	3.18	1.13
SE Tarim (Qiemo)	Oligocene/Miocene	19.9	18.9	2	4	0.66	0.13	2.25	12.71	-10.5
	Miocene/L. Pliocene	18.9	16.2	4	5	0.13	0.64	6.2	2.57	3.63
	L. Pliocene/U. Pliocene	16.2	18	5	7	0.64	1.07	3.24	2.26	0.98
Northern Tarim (Kuqa)	Oligocene/Miocene	21.7	21.9	4	9	0.13	0.99	0.38	2.23	-1.85
	Miocene/U. Miocene-Pliocene	21.9	20.4	9	7	0.99	0.794	3.13	2.16	0.97

μ_1 and μ_2: means of the first and second groups.
n_1 and n_2: numbers of samples in the first and second groups.
ν_1 and ν_2: variances of the first and second groups.
t_c: calculated t values, t_t: values from the standard t table.

ter. We first cut a flat surface, obtained a small piece (~0.1 mm^3) and mounted it with epoxy. Then, we polished the mount to expose carbonate sample, and analyzed the sample under Scanning Electronic Microscope to locate carbonate material. Finally,

TABLE 3

Sandstone Point Counting Results

Sample	Straigraphic Position (m)	Total Counts	Extra-basinal	Cement	Matrix	Pore	IGV	Extrabasinal/ Cement	Extrabasinal/ Total
95GC103 *	10	498	0	52	83	5	0.281	0.00	0.00
95GC129	2160	500	6	77	54	7	0.276	0.08	0.01
95GC132	2215	500	2	11	88	7	0.212	0.18	0.00
95GC134	2245	500	0	17	65	0	0.164	0.00	0.00
95GC135	2260	498	9	99	116	3	0.438	0.09	0.02
95GC136	3160	500	1	16	138	5	0.318	0.06	0.00
95GC137	3165	499	17	48	64	22	0.269	0.35	0.03
95GC138	4520	500	1	105	21	3	0.258	0.01	0.00
95GC139	5030	500	3	134	32	16	0.364	0.02	0.01
96RE100	20	500	4	136	59	42	0.474	0.03	0.01
96RE102	105	500	5	88	125	19	0.464	0.06	0.01
96RE103	125	500	0	40	130	1	0.342	0.00	0.00
96RE104	135	503	7	38	130	16	0.366	0.18	0.01
96RE105	310	505	6	43	86	14	0.283	0.14	0.01
96RE106	390	500	5	47	93	25	0.330	0.11	0.01
96RE107	525	500	2	27	130	36	0.386	0.07	0.00
96RE108	660	500	3	46	85	0	0.262	0.07	0.01
96RE109	740	530	0	57	70	0	0.240	0.00	0.00

* Samples 95GC103-139 were collected from Ganchaigou, and samples 96RE100-109 from Kashitashi.

TABLE 4

Mg/Ca and Sr/Ca Ratios of Samples from Ganchaigou

Sample	Stratigraphic Position (m)	Mg/Ca	Sr/Ca
95GC105-3	10	0.3956	0.0014
95GC110-1	415	0.0004	0.0012
95GC113-1	560	0.0060	0.0022
95GC114-1	610	0.0263	0.0016
95GC116-1	705	0.0091	0.0012
95GC117-1	730	0.0064	0.0008
95GC119-1	980	0.0088	0.0005
95GC122-1	1570	0.0007	0.0019
95GC123-1	1810	0.0022	0.0006
95GC125-1	1880	0.0039	0.0005
95GC127-1	2140	0.0085	0.0032
95GC128-1	2145	0.0080	0.0037
95GC130-1	2170	0.0042	0.0016

we analyzed the sample using SHRIMP-RG to obtain its $^{88}Sr/^{43}Ca$ and $^{25}Mg/^{43}Ca$ ratios, from which Sr/Ca and Mg/Ca ratios were respectively calculated.

STABLE ISOTOPE RESULTS

We present oxygen isotope results of eighty-six samples of carbonate from fluvial and lacustrine sediments, and paleosol carbonate from four localities in a 700,000 km^2 area of the Tarim and Qaidam basins (table 1). To facilitate interpretation of our analytical results, we plot our isotopic data against sample age in figure 3. Because of the lack of radiometric age control and uncertainty about the reliability of the paleontologic and paleomagnetic age assignments, we conservatively summed all samples at epoch level for each of the four localities and plotted epoch average ages. These group-average ages are plotted against the group-$\delta^{18}O$ values in figure 3. To test the legitimacy of this age-averaging procedure, we conducted a t-test (table 2), which indicates that for each section, our Eocene group-averages are statistically different from Oligocene group-averages (table 1). Similarly, in the three sections where sample numbers are sufficient, t-test results indicate that Miocene group-averages differ significantly from Pliocene group-averages. In contrast, Oligocene and Miocene group-averages are statistically indistinguishable, as visually suggested by figure 3. These results bolster our confidence in the age significance of our sample groupings and in turn suggest that paleontologic age assignments are meaningful at epoch level.

Our analyses reveal strikingly similar temporal patterns of syndepositional oxygen isotopic compositions in nonmarine strata over a region of 700,000 km^2 for the past 40 m.y (fig. 3). In addition, the recurrent temporal pattern of $\delta^{18}O$ values is consistently shifted by about +3 permil to +6 permil from southern Tarim basin to northern Tarim basin and finally up in altitude to the Qaidam basin on the leading edge of the Tibetan plateau. These results include both anticipated and unanticipated features, whose interpretation first requires consideration of present-day elevation, atmospheric circulation, temperature, and moisture sources and amounts. The region of our sampling, lying from 36° to 42°N, is dominated by upper level westerlies (Domros and Peng, 1984; Oort, 1984), with moisture provided principally by the Central Asia air mass (Araguas-Araguas and others, 1998) (fig. 4). Little moisture borne by these winds

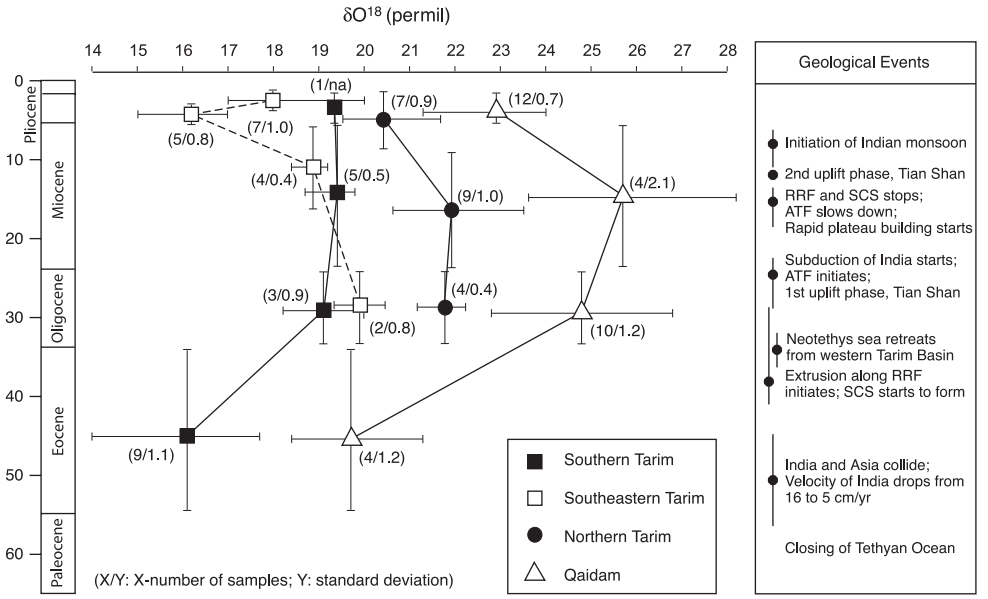

Fig. 3. Oxygen isotope composition (relative to SMOW) of Tertiary nonmarine carbonate of northern Tibet and Tarim Basin and correlation with major geological events in Asia. ATF-Altyn Tagh fault, RRF-Red River fault, SCS-South China Sea (Quade and others, 1989; Molnar and others, 1993; Hendrix and others, 1994; Dettman and others, 2001; Bullen and others, 2003; Yue and others, 2004a). Uncertainty bars for data: horizontal = total range of analytical values, vertical = uncertainty in biostratigraphic ages; Geologic events: filled circles = most probable ages, vertical bars = possible age ranges.

reaches the internally drained Tarim basin, which is surrounded by mountainous and plateau regions, reaching especially great altitudes around its western (windward) margin in the Karakorum (up to 7.8 km) and Tian Shan (up to 7.4 km) ranges. Mean annual temperature varies between 8°C to 12°C and mean annual precipitation in the region of northern Tibet and Tarim basin is <100 mm/yr, with greater than 50 percent occurring from June to August (Domros and Peng, 1984).

Few isotopic data exist for modern precipitation in the region, but extrapolation from IAEA data sites show that stable isotopic values have a north to south variation of –12 permil to –16 permil $\delta^{18}O$ from northern China to northern Tibet in the winter and –4 permil to –8 permil in the summer (Lawrence and White, 1991; Araguas-Araguas and others, 1998; Tian and others, 2003). No significant east to west gradients are documented for the region.

The seasonal pattern of the Central Asia air mass providing isotopically heavier precipitation in the summer relative to the winter exists over most of the area examined in this study. However, the far eastern section (Ganchaigou) examined here could also have been influenced by the South Pacific air mass, as the maximum extent of this air mass lies along the eastern edge of the Qaidam basin (Araguas-Araguas and others, 1998). In contrast to the Central Asia air mass, the South Pacific air mass provides moisture associated with summer monsoonal circulation. Monsoonal activity results in a contrasting seasonal isotopic pattern, with summer precipitation being isotopically lighter than winter precipitation. At the eastern margin of the Qaidam basin, precipitation from the summer monsoon is depleted in ^{18}O and D relative to winter precipitation by as much as ~4 permil (Araguas-Araguas and others, 1998).

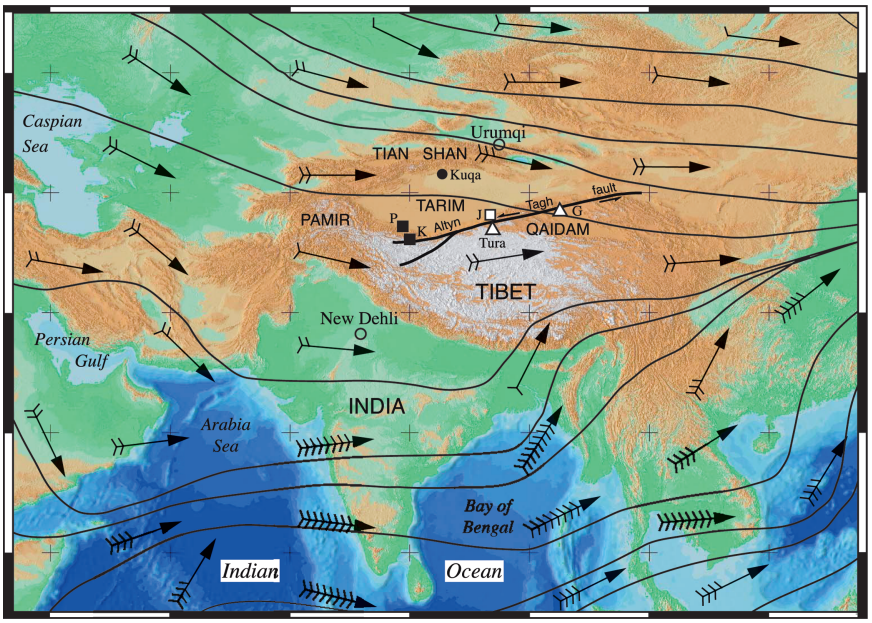

Fig. 4. Topography and transport vector field of water vapor of Tibet and adjacent regions during July, the summer monsoon season (Oort, 1984). Bold lines indicate direction of water vapor transportation. Arrows with barbs show the local strength of local water flux. Each barb represents an average transport of water vapor of 2 $ms^{-1} \cdot g \cdot kg^{-1}$. Oxygen isotope sampling locality symbols are the same as in figure 1. Abbreviations: G = Ganchaigou, J = Janggalsay, K = Kashitashi, P = Pianaman.

DISCUSSION

Evaluating the Isotopic Signal

We suggest that the observed shifts in oxygen isotope records are mainly due to the uplift of the Himalaya/Tibet system and its effects on paleoclimate. However, we recognize that several other factors could potentially affect the oxygen isotope values of the analyzed samples. These include: contamination by extrabasinal detrital carbonate, paleosalinity effects and burial diagenetic effects. We evaluate the potential influences of these effects on our isotopic signals in the following sections.

Contamination by extrabasinal carbonate grains.—Table 3 shows the extrabasinal detrital carbonate and carbonate cement contents of sandstone samples collected from the Ganchaigou and Kashitashi sections. For the Ganchaigou section, the average extrabasinal carbonate content is 0.8 percent (table 3), with a range from 0 to 3.4 percent. In contrast, the average carbonate cement content is 12.4 percent, 15 times more than the extrabasinal carbonate content. Similarly, the content of extrabasinal grains of Kashitashi section is 0.7 percent, with a range from 0 to 1.4 percent, whereas the average carbonate cement content is 11.5 percent (fig. 5A). This indicates that contamination from extrabasinal carbonate grains is unlikely, especially given the care we took in drilling our samples.

Evaporative effects.—Paleosalinity, fostered by extreme evaporative conditions, can have a large effect on oxygen isotope values of carbonate (Chivas and others, 1993). However, as shown in table 4 and figure 6, the Sr/Ca ratios of all the samples analyzed are low, suggesting low paleosalinity (Chivas and others, 1993). The increases in Sr/Ca ratio and inferred paleosalinity from Miocene to Pliocene do not indicate any effect on the oxygen isotope results because such an increase tends to increase $\delta^{18}O$, whereas all the sections show a decrease (fig. 3).

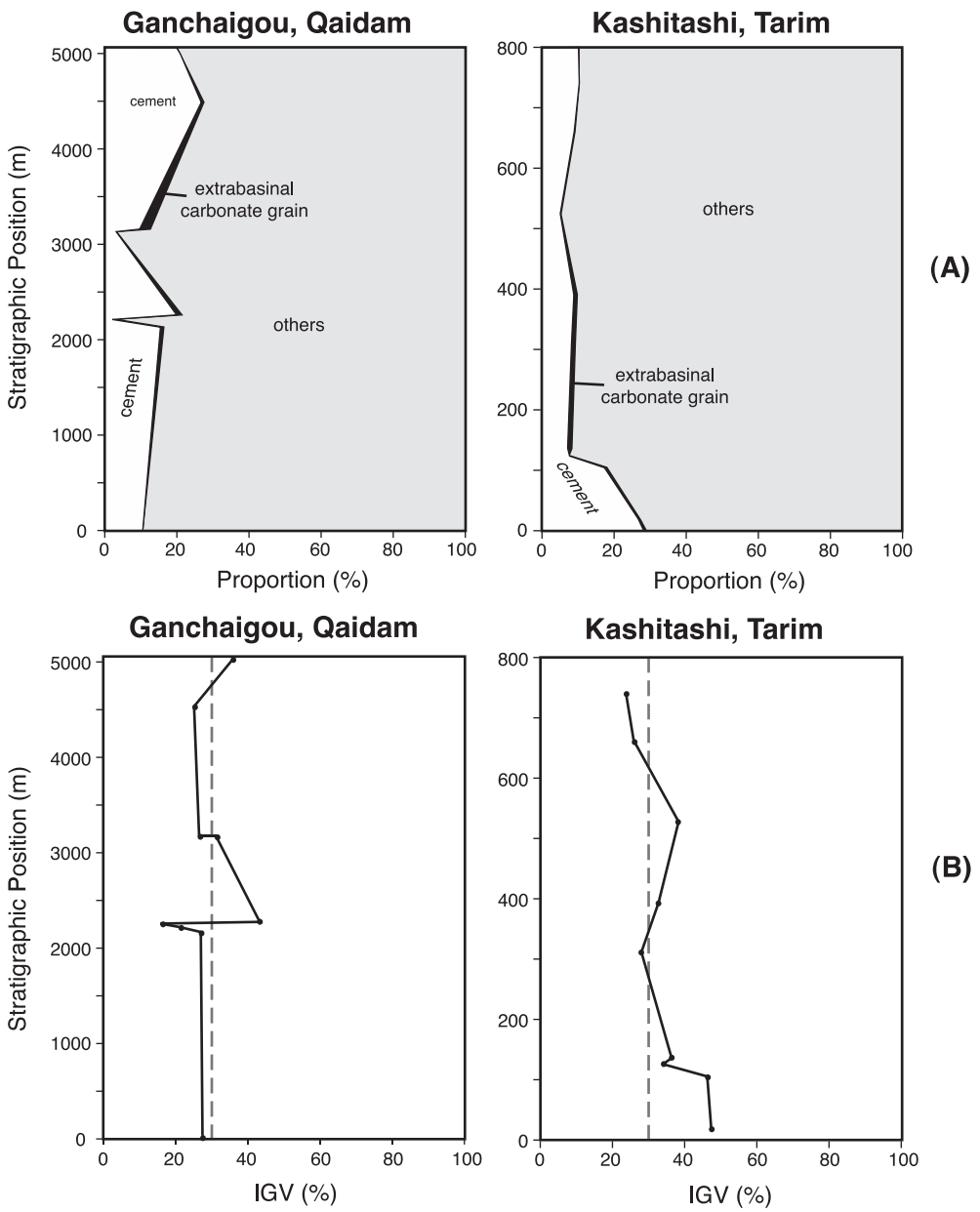

Fig. 5. (A). Relative abundance of calcite cement and extrabasinal carbonate grains in sandstone from Ganchaigou section, Qaidam basin and Kashtashi section. Southern Tarim, (B). Intergranular volume (IGV) of sandstone samples. Data are tabulated in table 3.

We do not dismiss the role that evaporation might play in the isotopic record presented here, particularly with regard to the large positive isotopic shift observed between Eocene and Oligocene rocks. As discussed later, we suggest that some of this increase could be due to increased aridity and evaporation as a result of the rise of the Himalaya-Tibet region. We do not have Sr/Ca and Mg/Ca ratios for the Eocene samples to compare with Oligocene samples to test this hypothesis, however.

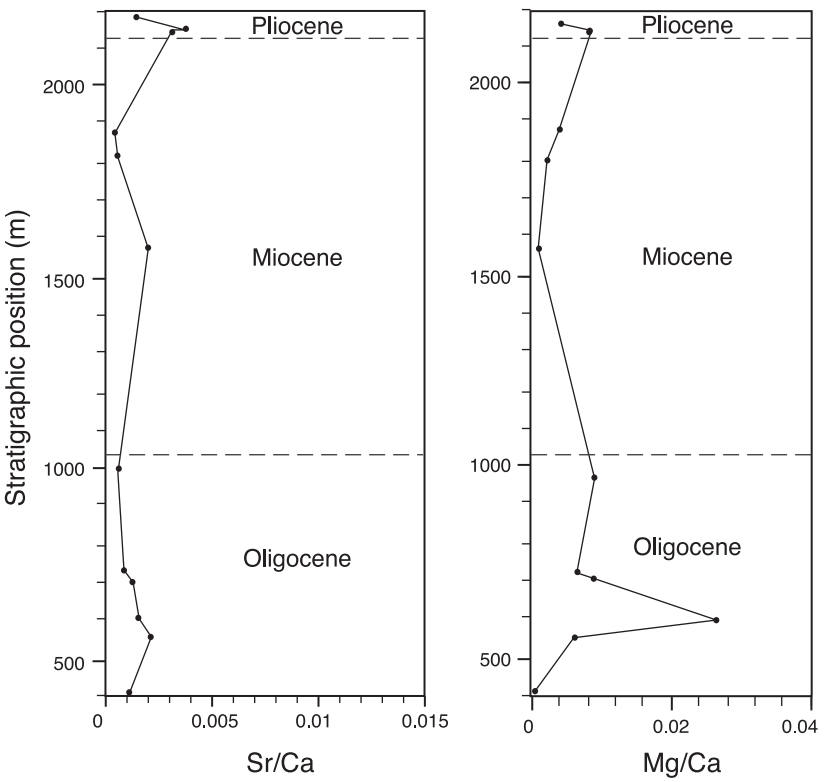

Fig. 6. Sr/Ca and Mg/Ca ratios plotted against stratigraphic position in the Ganchaigou section. Stratigraphic position is measured from the bottom of the section (Hanson, ms, 1999).

Burial Diagenetic Effects.—Burial diagenetic processes can alter the oxygen isotope composition of carbonate minerals. Diagenetic effects are considered to be minor in this study for two reasons. First, low Mg/Ca and Sr/Ca ratios in calcite reveal little dolomitization (table 4). For the six Oligocene samples, the Mg/Ca ratio is generally below 0.01, except for one sample whose ratio is around 0.03. For the Miocene samples, all the Mg/Ca ratios are lower than 0.004, while for the Pliocene samples the same ratios are lower than 0.008 (fig. 6). This is a strong indication that burial diagenetic effects were minimal.

Second, throughout the entire 5000 m section, the intergranular volume (Houseknecht, 1987; Paxton and others, 2002) of the Tertiary sandstone at Ganchaigou is uniformly around 30 percent (table 3, fig. 5B). The intergranular volume of the four samples lower in the section at Kashtashi is around 40 percent, whereas the other five samples from the upper section is around 30 percent. These high intergranular volume values indicate that cementation of sandstone was early and occurred at shallow burial depth, preventing the sandstone from further compaction (compare Houseknecht, 1987; Paxton and others, 2002). Petrographic examination of one-third of our sandstone samples reveals a spectrum of cementation, ranging from sparse, simple calcite cement, to more complicated cement stratigraphies involving calcite and clay with some framework grain replacement by calcite. The latter does indicate that a more detailed investigation of cement composition is warranted in future studies.

In addition, thermochronometric measures indicate that burial heating of the stratigraphic sections we sampled has in general been modest. In SE Tarim, vitrinite

reflectance = 0.5 to 0.6 for underlying Jurassic strata, with no apatite fission track resetting in Cenozoic samples (Hanson, ms, 1999); in southern Tarim basin, vitrinite reflectance = 0.48 for Eocene strata (Sobel, ms, 1995); and in Qaidam basin, vitrinite reflectance = 1.06 (Hanson, ms, 1999).

Paleoclimatic Interpretations

Most fundamentally, our data reveal a regionally consistent, temporally varying oxygen isotopic stratigraphic record across Tarim and Qaidam basins with a large positive isotope increase from Eocene to Oligocene. The explanation for the temporal isotopic shifts recorded in our data (fig. 3) must explain (1) an approximately 4 permil to 6 permil positive shift in oxygen isotope values from the Eocene to the Oligocene, (2) a relatively stable isotopic record during the Oligocene and Miocene, and (3) a 2 permil to 3 permil negative shift in oxygen isotope values in the late Miocene. In addition, explanations must account for the consistent shift in values between southern, southern/southeastern Tarim, northern Tarim and Qaidam basin localities. As indicated above, the isotopic records presented here are most likely the result of the combined effects of temperature, the isotopic composition of source waters, and aridity rather than burial diagenesis, as both low Mg/Ca ratios and high intergranular porosity values indicate (figs. 5 A, B and 6).

The isotopic records show strikingly similar trends in all four sections, despite great geographic separation, leading us to conclude that the isotopic signals primarily reflect surface source waters and regional climate. We therefore offer the following explanations, viewed in context of regional tectonic history, global climate modeling of the impact of plateau growth (Kutzbach and others, 1989; Ruddiman and Kutzbach, 1990; Kutzbach and others, 1993) and retreat of the Neotethyan sea from western Tarim basin in the middle Tertiary.

Eocene to Oligocene.—We suggest that the positive isotopic shift of 4 permil to 6 permil from the Eocene to the Oligocene ultimately results from initial uplift of the Himalaya in the Eocene and attendant reorganization of climate patterns. However, it is difficult to uniquely determine the cause of this isotopic shift because we know little about how initial rise of the Himalaya and Tibet in the Eocene affected the air masses and climate of this area.

Three reasonable possibilities could create an increase in isotope composition of precipitation associated with the rise of the Himalaya-Tibet region: increased aridity, increased temperature, and change in seasonality of precipitation. GCM models involving growth of the Himalaya-Tibet region predict increased aridity and an 8°C rise in temperature north of the Himalaya (Kutzbach and others, 1989; Ruddiman and Kutzbach, 1990; Prell and Kutzbach, 1992; Kutzbach and others, 1993). Although these predictions are useful in providing some constraints on the paleoclimate of this region, they do not account for the substantial northward movement of the Himalaya and related topographic evolution, and therefore should be used with caution. Taken at face value, an increase of 8°C would result in an increase in the oxygen isotope values of calcite by 2.8 permil. This estimate uses the fractionation of oxygen between calcite and water in this temperature range ($\sim -0.23‰/°C$; O'Neil and others, 1969) and the correlation between temperature and oxygen isotope values of precipitation ($\sim 0.58‰/°C$; Rozanski and others, 1993), resulting in a combined oxygen isotope change of $0.35‰/°C$.

Increased aridity would have enhanced evaporitic conditions and tended to increase the $\delta^{18}O$ values in groundwaters of the region. It is difficult to quantify how large this evaporitic effect might be with the current isotopic data set, as assessing evaporation requires having both hydrogen and oxygen isotopic data. Nevertheless evaporation can cause relatively large positive isotopic shifts. For example, by using combined oxygen and hydrogen isotope values of freshwater chert from Eocene lakes

in western North America, lakes similar to those studied here, increases of 10 permil can be attributed to evaporation alone (Abruzzese and others, 2005).

A change in seasonality to increased precipitation in the summer months could also cause a large positive shift in isotopic values. Presently, precipitation in the western Tarim region differs in oxygen isotope values by 12.8 permil from summer to winter, and nearly 80 percent of precipitation occurs during the summer months (Araguas-Araguas and others, 1998). Thus, an increase in summer precipitation could significantly increase the oxygen isotope values of groundwater.

Thus, we suggest that the combined effect of an increase in temperature, aridity, and amount of summer precipitation could result in the observed 4 permil increase in $\delta^{18}O$ values in the basins north of Tibet. To fully understand what caused the positive isotopic shift that we observe over a large area of northern Tibet will require more sophisticated GCM models that account for northward drift of the Himalayan-Tibet region. Nevertheless the isotopic inferences presented here are consistent with India-Asia collision in late Paleocene, a significant decrease in northward velocity of India in the late early Eocene (Patriat and Achache, 1984) and attendant uplift of the Himalaya-Tibet region driven by crustal shortening in the later Eocene (fig. 3).

In appealing to effects associated with early structural and topographic evolution of the Himalaya-Tibet, we think it unlikely that the positive shift of oxygen isotope values observed from Eocene to Oligocene in our sample set is the result of global climate change at the Eocene/Oligocene boundary. Other oxygen isotopic records for terrestrial rocks do not show a positive isotopic shift as we observe here. In fact, nonmarine rocks in the Basin and Range of North America show a decrease in oxygen isotope values from the Eocene to the Oligocene (Horton and others, 2004), and rocks along the Rocky Mountain Front Range show no change in oxygen isotope values from the Eocene to the Oligocene (Sjostrom and others, 2005).

The consistent 4 permil difference between Tarim and Qaidam samples seemingly indicates that significant topographic relief already existed between the southern Tarim basin and the current northeastern leading edge of the Tibetan plateau by sometime in the Eocene. Paleocene strata, scarce in the region, will need to be sampled in order to determine the timing of initial uplift and development of topographic relief between Qaidam basin and Tarim basin. This structural/topographic boundary is currently defined by the Altyn Tagh fault (fig. 1), a major strike-slip fault considered in many models to be associated with collisional extrusion tectonics (Yue and Liou, 1999; Tapponnier and others, 2001). Our results permit the inference that faulting along this trend produced significant relief by Eocene time, even though piercing point relations suggest that significant strike-slip did not commence until sometime in the Oligocene (Yue and others, 2004a) (fig. 3).

Late Miocene.—We propose three alternative explanations for the negative isotopic shift consistently recorded in upper Miocene strata at all four localities: (1) The retreat of the easternmost arm of the Neotethyan sea from Tarim basin by the early Miocene likely shifted central Asian climate from relatively temperate to continental and thereby played a role as important to climate as plateau uplift, as has been predicted by modeling involving patterns of land-sea distribution (Ramstein and others, 1997). The loss of a nearby moisture source for precipitation would cause $\delta^{18}O$ of precipitation to decrease. Using the empirical longitudinal effect of 0.002 permil per kilometer (Criss, 1999), retreat of the sea by 1000 km to the west, consistent with facies relations indicating marine regression from the middle of Tarim basin to beyond its western limit (Zhou and Chen, 1990), would produce a 2 permil lowering of isotopic values. (2) An intriguing alternative possibility is that the Tibetan plateau reached a critical threshold of elevation at this time. Molnar and others (1993) noted that subtropical air below the trade cumulus boundary at about 2 to 3 km is relatively moist. If Tibet were

lower than 2 to 3 km during the Eocene, it is possible that moist air flowed over the mountains from the south without moisture loss, increasing the $\delta^{18}O$ values of precipitation to the region north of Tibet. Assuming Tibet underwent rapid uplift circa 10 to 7 Ma (fig. 3) as has been suggested (Quade and others, 1989), then this rise in elevation might have cut off the southern (Indian Ocean) heavy moisture source and resulted in a lowering of isotopic values north of Tibet. Consistent with this interpretation, isotopic values become 'heavier' south of the Himalaya during this time frame (Quade and others, 1989; Stern and others, 1997; Dettman and others, 2001) perhaps indicating that all moisture came from the Indian Ocean to the south and the loss of communication with isotopically 'lighter' northern air masses (Stern and others, 1997). Similarly, Dettman and others (2003) recently attributed a significant isotope shift at 12 Ma in sediments of the Linxia basin, NE Tibetan plateau to uplift of the plateau and resulting aridification after loss of southern moisture sources. (3) The initial Cenozoic reactivation and rise of the Tian Shan during the late Oligocene and Miocene (figs. 1, 3), indicated by thermochronologic studies (Hendrix and others, 1994; Dumitru and others, 2001; Bullen and others, 2003), would have deflected westerly atmospheric flow even further to the north while creating a rain shadow in Tarim basin to the south, as is currently evident in contrasting vegetation patterns from the forested northern slopes to the barren southern slopes of the modern Tian Shan. A 2 permil shift such as observed in our data (fig. 3) could be created by a 0.7 km increase in surface elevation in the Tian Shan (using the isotopic lapse rates of Poage and Chamberlain, 2001). Increased salinity of surface waters does not account for the observed negative Miocene-Pliocene shift, because an increase in salinity would yield a positive shift.

Note that Chen and others (2002) also sampled our SE Tarim basin section, in part during a joint field season in 1996, and obtained isotopic results consistent with ours for Oligocene through Pliocene strata. However, they also sampled an interval they assigned as Paleocene/Eocene, contrary to the Xinjiang provincial geologic map and other published references (Zhou and Chen, 1990; Xinjiang Bureau of Geology and Mineral Resources, 1993; Yin and others, 2002; Yue and others, 2004a) (and our interpretation in this paper). If their Paleocene/Eocene strata are instead considered Oligocene, then the average of their Oligocene isotopic measurements is comparable to ours.

CONCLUDING REMARKS

In summary, a regionally consistent record of oxygen isotopic composition exists in Eocene-Pliocene strata of the northern Tibetan Plateau and the vast Tarim basin beyond to the north. This record includes a significant positive isotopic shift from Eocene to Oligocene, perhaps reflecting early development of Himalaya-Tibet topography associated with the collision of India and attendant aridification related to loss of moisture reaching central Asia. A consistent separation of the northern Tibet (Qaidam basin) and southern Tarim basin isotopic curves may indicate that topographic relief comparable to that of the present day already existed by the Eocene, driven by early phases of collisional crustal thickening. The relatively constant isotopic values from the Oligocene to the late Miocene suggest that the climate of northern Tibet was relatively stable during this time interval, a result consistent with other isotopic records in basins on the far NE margin of Tibet (Dettman and others, 2003). A subsequent Miocene isotopic shift in the opposite (negative) direction generally coincided with, and presumably was related to, retreat of the Neotethyan Sea from the Tarim basin, as well as enhanced elevation of the Himalaya/Tibetan plateau region and the rise of the Tian Shan, which diverted moisture-bearing Westerlies and deepened aridity in the Tarim basin and the northern Tibetan plateau.

ACKNOWLEDGMENTS

We thank R. B. Dunbar for reviewing an early version of the paper. Peter Molnar and Jay Quade provided valuable reviews of the submitted manuscript. This work is supported by U.S. National Science Foundation grants (EAR-0207364, EAR-0207115).

References

Abruzzese, M. J., Waldbauer, J. R., and Chamberlain, C. P., 2005, Oxygen and hydrogen isotope ratios in freshwater chert as indicators of ancient climate and hydrologic regime: Geochimica et Cosmochimica Acta, v. 69, p. 1377–1390.

Araguas-Araguas, L., Froehlich, K., and Rozanski, K., 1998, Stable isotope composition of precipitation over southeast Asia: Journal of Geophysical Research, v. 103, p. 28,721–28,742.

Bullen, M. E., Burbank, D. W., and Garver, J. I., 2003, Building the northern Tien Shan; integrated thermal, structural, and topographic constraints: Journal of Geology, v. 111, p. 149–165.

Cerling, T. E., 1984, The stable isotopic composition of modern soil carbonate and its relationship to climate: Earth and Planetary Science Letters, v. 71, p. 229–240.

Chamberlain, C .P., and Poage, M. A., 2000, Reconstructing the paleotopography of mountain belts from the isotopic composition of authigenic minerals: Geology, v. 28, p. 115–118.

Chen, Z. L., Wang, X. F., Feng, X. H., Wang, C. Q., and Liu, J., 2002, New evidence from stable isotopes for the uplift of mountains in northern edge of the Qinghai-Tibetan Plateau: Science in China Series B-Chemistry, v. 45, supplement S, p. 1–10.

Chivas, A. R., De Decker, P., Cali, J. A., Chapman, A., Kiss, E., and Shelley, J. M. G., 1993, Coupled stable-isotope and trace-element measurements of lacustrine carbonates as paleoclimatic indicators, *in* Swart, P. K., Lohmann, K. C., Mckenzie, J., and Savin, S., editors, Climate change in continental isotopic records: American Geophysical Union Monograph 78, p. 113–121.

Criss, R. E., 1999, Principles of stable isotope distribution: New York, Oxford University Press, 254 p.

Dettman, D. L., Kohn, M. J., Quade, J., Ryerson, F. J., Ojha, T. P., and Hamidullah, S., 2001, Seasonal stable isotope evidence for a strong Asian monsoon throughout the past 10.7 m.y.: Geology, v. 29, p. 31–34.

Dettman, D. L., Fang, X., Garzione, G. N., and Li, J., 2003, Uplift-driven climate change at 12 Ma: a long ^{18}O record from the NE margin of the Tibetan plateau: Earth and Planetary Science Letters, v. 214, p. 267–277.

Domros, M., and Peng, G., 1984, The Climate of China: New York, Springer-Verlag, 360 p.

Dumitru, T. A., Zhou, D., Chang, E., Graham, S. A., Hendrix, M. S., Sobel, E. R., and Carroll, A. R., 2001, Uplift, exhumation and deformation in the Chinese Tian Shan, *in* Hendrix, M. S. and Davis, G. A., editors, Paleozoic and Mesozoic tectonic evolution of central and eastern Asia—from continental assembly to intracontinental deformation: Geological Society of America Special Paper 194, p. 71–99.

Garzione, C. N., Dettman, D. L., Quade, J., Decelles, P. G., and Butler, R. F., 2000, High times on the Tibetan Plateau: Paleoelevation of the Thakkhola graben, Nepal: Geology, v. 28, p. 339–342.

Gilder, S., Chen, Y., and Sen, S., 2001, Oligo-Miocene magnetostratigraphy and rock magnetism of the Xishuigou section, Subei (Gansu Province, western China) and implications for shallow inclination in central Asia: Journal of Geophysical Research, v. 106, p. 30505–30521.

Graham, S. A., Hendrix, M. S., Wang, L. B., and Carroll, A. R., 1993, Collisional successor basins of western China: impact of tectonics inheritance of sand composition: Geological Society of America Bulletin, v. 105, p. 323–344.

Gu, S. S., Xu, W., Xue, C., Di, S. Q., Yang, F., Di., H. S., and Zhao, D. N., 1990, Petroleum Geology of China: Vol. 14: Beijing, Petroleum Industrial Press, 483 p.

Hanson, A. D., ms, 1999, Organic geochemistry and petroleum geology, tectonics and basin analysis of southern Tarim and northern Qaidam basins, northwest China: Ph.D. thesis, Stanford University, Stanford, 388 p.

Hendrix, M. S., Dumitru, T. A., and Graham, S. A., 1994, Late Oligocene-early Miocene unroofing in the Chinese Tian Shan; an early effect of the India-Asia collision: Geology, v. 22, p. 487–490.

Horton, T. E., Sjostrom, D. J., Abruzzese, M. J., Poage, M. A., Waldbauer, J. R., Hren, M., Wooden, J., and Chamberlain, C. P., 2004, Spatial and temporal variation of Cenozoic surface elevation in the Great Basin and Sierra Nevada: American Journal of Science, v. 304, p. 862–888.

Houseknecht, D. W., 1987, Assessing the relative importance of compaction processes and cementation to reduction of porosity in sandstones: AAPG Bulletin, v.71, p. 633–642.

Kutzbach, J. E., Guetter, P. J., Ruddiman, W. F., and Prell, W. L., 1989, Sensitivity of climate to late Cenozoic uplift in southern Asia and the American West; numerical experiments: Journal of Geophysical Research, v. 94, p. 18,393–18,407.

Kutzbach, J. E., Prell, W. L., and Ruddiman, W. F., 1993, Sensitivity of Eurasian climate to surface uplift of the Tibetan Plateau: Journal of Geology, v. 101, p. 177–190.

Lawrence, J. R., and White, J. W. C., 1991, The elusive climate signal in the isotope composition of precipitation, *in* Taylor, H. P., O'Neil, J. R., and Kaplan, I. R., editors, Stable isotope geochemistry: A tribute to Samuel Epstein: Geochemical Society Special Publication 3, p. 169–185.

Lockley, M. G., Ritts, B. D., and Leonardi, G., 1999, Mammal track assemblages from the early Tertiary of China, Peru, Europe and North America: Palaios, v. 14, p. 398–404.

Mack, G. H., and James, W. C., 1992, Paleosols for Sedimentologists: Cincinnati, Geological Society of America, 127 p.

McKenzie, J. A., and Hollander, D. J., 1993, Oxygen-isotope record in recent carbonate sediments from Lake Greifen, Switzerland (1750–1986): Application of continental isotopic indicator for evaluation of changes in climate and atmospheric circulation patterns, *in* Swart, P. K., Lohmann, K. C., McKenzie, J., and Savin, S., editors, Climate change in continental isotopic records: American Geophysical Union Monograph 78, p. 101–112.

Molnar, P., England, P. C., and Martinod, J., 1993, Mantle dynamics, uplift of the Tibetan Plateau, and the Indian monsoon: Reviews of Geophysics, v. 31, p. 357–396.

O'Neil, J. R., Clayton, R. N., and Mayeda, T. K., 1969, Oxygen isotope fractionation in divalent metal carbonates: Journal of Chemical Physics, v. 51, p. 5547–5558.

Oort, A. H., 1984, Variability of the hydrological cycle in the Asian monsoon region, *in* Ye, D., Fu, C., Chao, J., and Yoshino, M., editors, The climate of China and global climate: Beijing, China Ocean Press and Springer-Verlag, p. 270–285.

Patriat, P., and Achache, J., 1984, India Eurasia collision chronology has implications for crustal shortening and driving mechanism of plates: Nature, v. 311, p. 615–621.

Paxton, S. T., Szabo, J. O., Ajdukiewicz, J. M., and Klimentidism, R. E, 2002, Construction of an intergranular volume compaction curve for evaluating and predicting compaction and porosity loss in rigid-grain sandstone reservoirs: AAPG Bulletin, v. 86, p. 2047 –2067.

Poage, M. A., and Chamberlain, C. P., 2001, Empirical relationships between elevation and the stable isotope composition of precipitation and surface waters; considerations for studies of paleoelevation change: American Journal of Science, v. 301, p. 1–15.

Prell, W. L., and Kutzbach, J. E., 1992, Sensitivity of the Indian monsoon to forcing parameters and implications for its evolution: Nature, v. 360, p. 647–652.

Qinghai Bureau of Geology and Mineral Resources, 1991, Regional Geology of Qinghai Province: Beijing, Geological Publishing House, 662 p.

Quade, J., Cerling, T. E., and Bowman, J. R., 1989, Development of the Asian monsoon revealed by marked ecologic shift in the latest Miocene of northern Pakistan: Nature, v. 342, p. 117–119.

Ramstein, G., Fluteau, F., Besse, J., and Joussaume, S., 1997, Effect of orogeny, plate motion and land-sea distribution on Eurasian climate change over the past 30 million years: Nature, v. 366, p. 788–795.

Retallack, G. J., 1990, Soils of the Past: an Introduction to Paleopedology: London, Unwin Hyman, 520 p.

Rieser, A. B., Bojac, A. V., Neubauer, F., Genser, J., Friedl, G., Liu, Y., and Ge, X. H., 2003, Cenozoic climate evolution of northeastern Tibet: Carbon and Oxygen isotope results from Qaidam basin, western China: Eos, v. 84, p. F877.

Ritts, B. D., ms, 1998, Mesozoic tectonics and sedimentation, and petroleum systems of the Qaidam and Tarim Basins, NW China: Ph.D. thesis, Stanford University, Stanford, 691 p.

Ritts, B. D., and Biffi, U., 2000, Magnitude of post-Middle Jurassic (Bajocian) displacement on the Altyn Tagh fault, NW China: Geological Society of America Bulletin, v. 112, p. 61–74.

Rowley, D. B., Pierrehumbert, R. T., and Currie, B. S., 2001, A new approach to stable isotope-based paleoaltimetry: implications for paleoaltimetry and paleohypsometry of the High Himalaya since the late Miocene: Earth and Planetary Science Letters, v. 188, p. 253–268.

Rozanski, K., Araguas-Araguas, L., and Gonfiantini, R., 1993, Isotopic patterns in modern global precipitation, *in* Swart, P. K., Lohmann, K. C., McKenzie, J., and Savin, S., editors, Climate change in continental isotopic records: American Geophysical Union Monograph 78, p. 1–36.

Ruddiman, W. F., and Kutzbach, J. E., 1990, Late Cenozoic uplift and climate change: Transactions of the Royal Society of Edinburgh: Earth Sciences, v. 81, p. 301–314.

Sjostrom, D.J., Hren, M.T., Horton, T.W., Waldbauer, J.R., and Chamberlain, C.P., 2005, Stable isotopic evidence for an early Tertiary elevation gradient in the Great Plains - Rocky Mountain region, in Willet, S., Hovius, N., Fisher, D., and Brandon, M., editors, Tectonics, Climate, and Landscape Evolution: Geological Society of America, Penrose Special Paper.

Smith, T. M., and Dorobeck, S. L., 1993, Early Mississippian climate change: Evidence from meteoric calcite, *in* Swart, P. K., Lohmann, K. C., McKenzie, J., and Savin, S., editors, Climate change in continental isotopic records: American Geophysical Union Monograph 78, p. 77–88.

Sobel, E., ms, 1995, Basin analysis and apatite fission-track thermochronology of the Jurassic-Paleogene southwest Tarim basin, NW China: Ph.D. thesis, Stanford University, Stanford, 308 p.

Stern, L. A., Chamberlain, C. P., Reynolds, R. C., and Johnson, G. D., 1997, Oxygen isotope evidence of climate change from pedogenic clay minerals in the Himalayan models: Geochimica et Cosmochimica Acta, v. 61, p. 731–744.

Sun, J. M., Zhu, R. X., and Bowler, J., 2004, Timing of the Tianshan Mountains uplift constrained by magnetostratigraphic analysis of molasse deposits: Earth and Planetary Science Letters, v. 219, p. 239–253.

Tapponnier, P., Xu, Z., Roger, F., Meyer, B., Arnaud, N., Wittlinger, G., and Yang, J., 2001, Oblique stepwise rise and growth of the Tibet Plateau: Science, v. 294, p. 1671–1677.

Tian, L., Yao, T., Schustr, P. F., White, J. W. C., Ichiyangi, K., Pendall, E., Pu, J., and Yu, W., 2003, Oxygen-18 concentrations in recent precipitation and ice cores on the Tibetan Plateau: Journal of Geophysical Research, v. 108, p. 16-1–16-10.

Wang, H. Z., compiler, 1985, Atlas of the Paleogeography of China: Beijing, Cartographic Publishing House, 143 p.

Wang, X., Wang, B., Qiu, Z., Xie, G., Xie, J., Downs, W., Qiu, Z., and Deng, T., 2003, Danghe area (western Gansu, China) biostratigraphy and implications for depositional history and tectonics of northern Tibetan Plateau: Earth and Planetary Science Letters, v. 208, p. 253–269.

Xinjiang Bureau of Geology and Mineral Resources, 1993, Regional Geology of Xinjiang Uygur Autonomous Region: Beijing, Geological Publishing House, 841 p.

Yang, F., Tang, W., Wei, J., Fu, Z., and Liang, S., 1994, Tertiary in Petroliferous Regions of China, Volume II: The Northwestern Region of China: Beijing, Oil Industrial Publishing House, 253 p.

Yin, A., Rumelhart, P., Butler, R., Cowgill, E., Harrison, T. M., Foster, D. A., Ingersoll, R. V., Zhang, Q., Zhou, Z., Wang, X. F., Hanson, A., and Raza, A., 2002, Tectonic history of the Altyn Tagh fault system in northern Tibet inferred from Cenozoic sedimentation: Geological Society of America Bulletin, v. 114, p. 1257–1295.

Yue, Y. J., and Liou, J. G., 1999, A two-stage model for the Altyn Tagh fault, China: Geology, v. 27, p. 227–230.

Yue, Y. J., Ritts, B. D., Graham, S. A., Wooden, J. L., Gehrels, G. E., and Zhang, Z. C., 2004a, Slowing extrusion tectonics: Lowered estimate of the post-Early Miocene slip rate along the Altyn Tagh fault: Earth and Planetary Science Letters, v. 217, p. 111–122.

Yue, Y. J., Ritts, B. D., Hanson, A. D., and Graham, S. A., 2004b, Sedimentary evidence against large-slip translation along the Northern Altyn Tagh fault, NW China: Earth and Planetary Science Letters, v. 228, p. 311–323.

Zheng, H. B., Powell, C. M., An, Z. S., Zhou, J., and Dong, G. R., 2000, Pliocene uplift of the northern Tibetan Plateau: Geology, v. 28, p. 715–718.

Zhou, Z., and Chen, P., 1990, Biostratigraphy and geologic evolution of Tarim: Beijing, Science Press, 366 p.